J Therm Anal Calorim (2012) 107:241–248
DOI 10.1007/s10973-011-1537-2

Sulfation behavior of white mud from paper manufacture as SO_2 sorbent at fluidized bed combustion temperatures

Yingjie Li · Rongyue Sun · Jianli Zhao · Kuihua Han · Chunmei Lu

Received: 5 March 2011 / Accepted: 23 March 2011 / Published online: 8 April 2011

Abstract The calcination characteristics, sulfation conversion, and sulfation kinetics of a white mud from paper manufacture at fluidized bed combustion temperatures were investigated in a thermogravimetric analyzer. Also, the comparison between the white mud and the limestone in sulfation behavior and microstructure was made. Although the white mud and the limestone both contain lots of $CaCO_3$, they are different in the alkali metal ions content and microstructure. It results in a marked difference in sulfation behavior between the white mud and the limestone. The CaO derived from white mud achieves the maximum sulfation conversion of 83% at about 940 °C which is 1.7 times higher than that derived from limestone at about 880 °C. The shrinking unreacted core model is appropriate to analyze the sulfation kinetics of the white mud. The chemical reaction activation energy E_a and the activation energy for product layer diffusion E_p for the sulfation of the white mud are 44.94 and 55.61 kJ mol^{-1}, respectively. E_p for the limestone is 2.8 times greater than that for the white mud. The calcined white mud possesses higher surface area than the calcined limestone. Moreover, the calcined white mud has more abundant pores in 4–24 nm range which is almost optimum pore size for sulfation. It indicates that the microstructure of the white mud is beneficial for SO_2 removal.

Keywords White mud · Sulfation behavior · SO_2 sorbent · Fluidized bed combustion temperatures

Y. Li (✉) · R. Sun · J. Zhao · K. Han · C. Lu
School of Energy and Power Engineering, Shandong University, No. 17923 Jingshi Road, Jinan 250061, China
e-mail: liyj@sdu.edu.cn

Introduction

Over the past 30 years, several processes have been proposed and developed for the removal of SO_2 from various exhausts. There is still no universally accepted solution to this problem. The implementation of new and more stringent regulations for the control of environmental pollution has encouraged the search for more efficient desulfurization processes [1, 2]. SO_2 in situ capture using calcium-based sorbents such as limestone and dolomite during coal combustion in circulating fluidized bed (CFB) boiler is a competitive process for industrial boilers[3, 4], due to the moderate desulfurization efficiency and low capital and operating costs [5–8]. Unfortunately, efficiency of this process is limited and limestone utilization in the range of 30–45% is not uncommon [5]. Due to larger size of CFB boilers (600–800 MWe) development [9], the consumption of limestone for SO_2 in situ capture will increase. Also, the exploit of the limestone mine will be improved. It will result in the aggravation of environmental destruction.

In China, lots of calcium-based industrial wastes such as carbide slag, red mud, white mud, and steel slag containing $CaCO_3$ or $Ca(OH)_2$ are produced from chemical industry (e.g., poly (vinyl chloride) as a raw material), alumina industry, paper manufacture industry, and steel industry, respectively every year [10]. It is an interesting and challenging topic to recycle the industrial wastes.

Recently, the industrial wastes were investigated as coagulant, sorbent, catalyst, and so on [11, 12]. Yamada and Harato [13] reported a study for SO_2 removal using red mud slurry as sorbent in laboratory. Fan et al. [14] reported on the work for coal gas desulfurization. They prepared a fixed-bed reactor using mixed clay with red mud in laboratory-scale and bench-scale operation. The results revealed that the red mud possessed good performance

with respect to both H_2S capture capacity and durability. Cheng et al. [15] investigated that the SO_2 capture capacity of some industrial wastes including calcium carbide residue, brine sludge, and white lime mud in fixed-bed reactor for simulating the desulfurization in pulverized coal-fired boiler at 1000–1600 °C. They found that combined industrial wastes and limestone could achieve the desulfurization efficiency above 45.8% at 1200 °C. It is easy to found that the mentioned above are the research on the industrial wastes as H_2S sorbent, SO_2 sorbent in a wet flue gas scrubbing process and in pulverized coal-fired boiler above 1000 °C, but these reports do not involve the typical fluidized bed combustion temperatures (800–950 °C).

The white mud is ordinarily abandoned from the paper manufacture and chlor-alkali plants. The white mud could be used as the soil nutrient amendment [16] and sorbent for the removal of an anionic dye [17]. It is mainly composed of $CaCO_3$ and possesses more impurities such as NaO, K_2O, Fe_2O_3, and SiO_2 than the natural limestone. These impurities have possibly important effects on the sulfation behavior of the white mud. Laursen et al. [18, 19] found that the addition of alkali metal ions improved the sulfur capture capacity of limestone. Siagi et al. [20] reported that the presence of Fe_2O_3 had a positive effect on the performance of the calcium-based sorbent during SO_2 capture. Therefore, the sulfation behavior of the white mud may be complicate, compared with the limestone. However, the sulfation behavior and kinetics of the white mud as SO_2 sorbent at fluidized bed combustion temperatures have seldom been investigated.

It is the aim of this study to research the calcination characteristics, sulfation conversion, sulfation kinetics, and microstructure of the white mud from paper manufacture at the fluidized bed combustion temperatures.

Experimental

A kind of white mud was sampled from a paper mill in Jinan, China. And a kind of limestone from Jinan was employed to compare the sulfation behavior with the white mud. The chemical compositions of the two sorbents are presented in Table 1. The particle size distributions of the white mud and limestone range from 0.105 to 0.3 mm.

The calcination experiments of the two sorbents were performed in a thermogravimetric analyzer (TGA) from Mettler-Toledo Inc. The mass of the sample was 10 ± 0.1 mg. The furnace was first heated with a scanning rate of 30 °C min^{-1} to a calcination temperature which was chosen from 850 to 1050 °C. When the TGA temperature reached the specified value, the sample was put in the TGA under a pure N_2 atmosphere.

In order to conveniently study the sulfation behavior of the white mud and the limestone, 3 g of each sorbent was calcined under a pure N_2 atmosphere in a fixed-bed reactor before putting in the TGA. The calcination temperature was the same as that in TGA and the calcination time is 10 min. The sulfation experiments of 10 ± 0.1 mg of the calcined sorbent from the fix-bed reactor were done in the TGA. The sulfation temperature in the TGA is the same as the calcination temperature in the fixed-bed reactor. A gas mixture containing 0.13 mol m^{-3} of SO_2, 2.23 mol m^{-3} of O_2, 6.7 mol m^{-3} of CO_2 and N_2 as an equilibrium gas was allowed to pass through the sorbents with a flow rate of 120 mL min^{-1}. The sulfation conversions of CaO derived from sorbents were calculated as follows:

$$X = \frac{(m_{\text{sul}} - m_1) \cdot M_{\text{CaO}}}{m_1 \cdot A \cdot (M_{\text{CaSO}_4} - M_{\text{CaO}})} \quad (1)$$

where X is sulfation conversion of CaO derived from sorbent, %; m_0 is initial sorbent mass, mg; m_1 is calcined sorbent mass, mg; m_{sul} is sulfated sorbent mass, mg; A is CaO mass fraction in calcined sorbent, %. M_{CaO} and M_{CaSO_4} is molecular mass of CaO and $CaSO_4$, mg mol^{-1}.

The surface areas and pore size distributions of the calcined sorbents sampled from the fixed-bed were analyzed by Quantachrome Poremaster-60 GT mercury intrusion porosimeter.

Results and discussion

Calcination characteristics

Figure 1 shows the effect of calcination temperature on calcination behavior of the white mud and the limestone. The mass loss and mass loss rate are used to describe the calcination behavior of the white mud and the limestone. Mass loss and mass loss rate are defined as follows.

$$W = \frac{m_{\text{cal}}}{m_0} \quad (2)$$

$$r_W = \frac{\mathrm{d}W}{\mathrm{d}t} \quad (3)$$

Table 1 The chemical compositions of white mud and limestone in wt%

Sample	SiO_2	Al_2O_3	Fe_2O_3	CaO	MgO	SO_3	Na_2O	K_2O	Others	LOI
White mud	10.7	0.86	0.72	48.55	1.89	0.00	0.42	0.63	0.87	35.36
Limestone	2.10	0.46	0.05	51.60	2.50	0.00	0.00	0.00	0.29	43.00

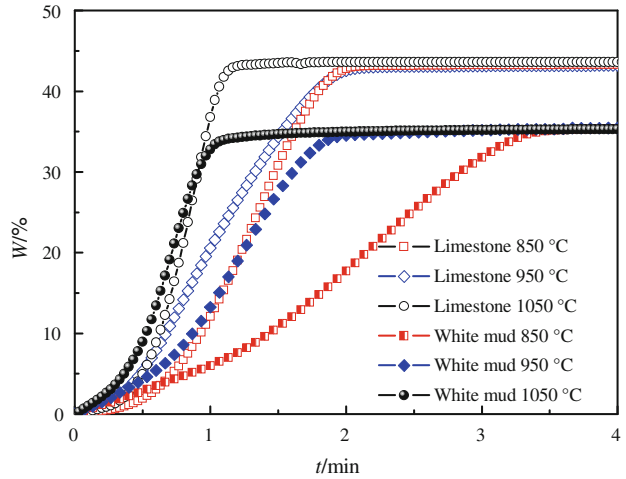

(a) Weight loss

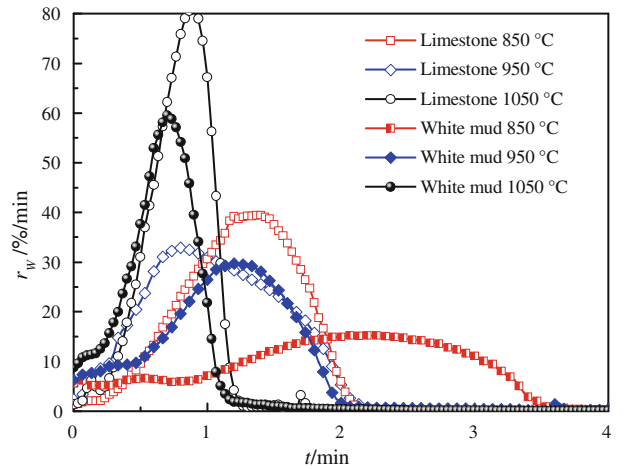

(b) Weight loss rate

Fig. 1 Calcination behavior of white mud and limestone at the different calcination temperatures. **a** Mass loss and **b** Mass loss rate

where W is mass loss, %; m_{cal} is mass of sorbent at any reaction time during calcination process, mg; r_W is mass loss rate, % min^{-1}; and t is reaction time, s.

The white mud and the limestone are completely decomposed at the range of 850–1050 °C as demonstrated in Fig. 1a. The ultimate mass loss for the white mud and the limestone is 43 and 35%, respectively. That is because white mud contains more impurity instead of $CaCO_3$ than the limestone. The result is in accordance with XRF analysis for the two sorbents as seen in Table 1. The complete decomposition time of the two sorbents becomes shorter with the calcination temperature. The complete decomposition time of the white mud at 850 °C is almost twice as long as that of the limestone at 850 °C, however, that of the former above 850 °C is similar to that of the latter at the same calcination temperature. Therefore, the calcination temperature above 850 °C is beneficial to the rapid decomposition of the white mud. The maximum mass loss rate of the white mud is lower than that of the limestone as shown in Fig. 1b. The difference in calcination behavior of the white mud and the limestone is attributed to their different components.

Sulfation behavior

Figures 2 and 3 displays the sulfation conversions of CaO derived from the white mud and the limestone, respectively, at the different sulfation temperature and reaction time. CaO derived from the white mud exhibits the maximum sulfation conversion of 83% at about 940 °C, and the sulfation conversion can reach above 76% at the range of 890–980 °C. CaO derived from the limestone achieves the highest conversion of 50% at approximately 880 °C and it can retain higher conversion above 45% at 850–920 °C

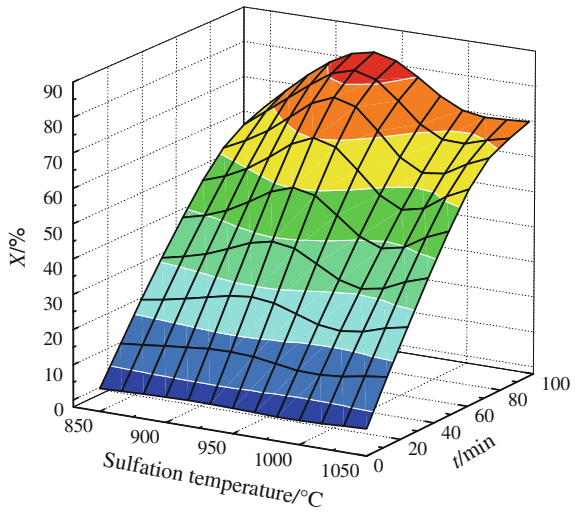

(a) Surface plot

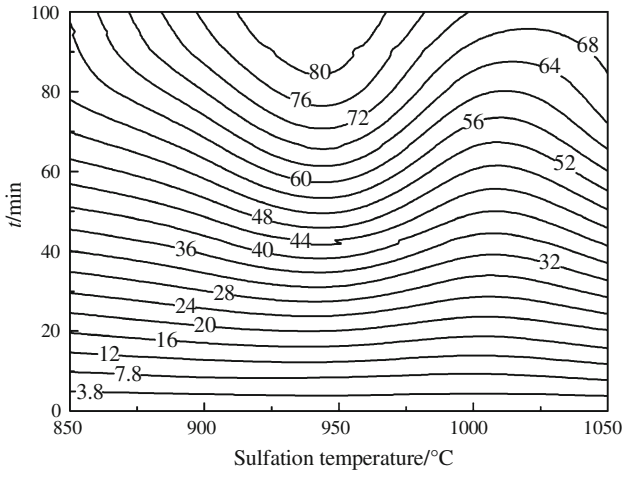

(b) Contour plot

Fig. 2 Effect of sulfation temperature and reaction time on sulfation conversion of white mud. **a** Surface plot and **b** Contour plot

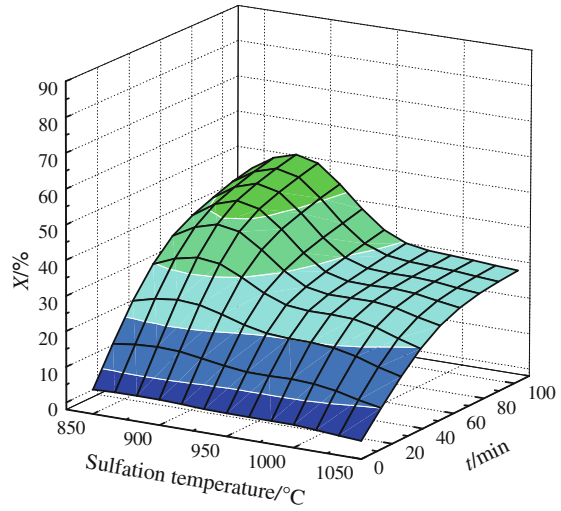

(a) Surface plot

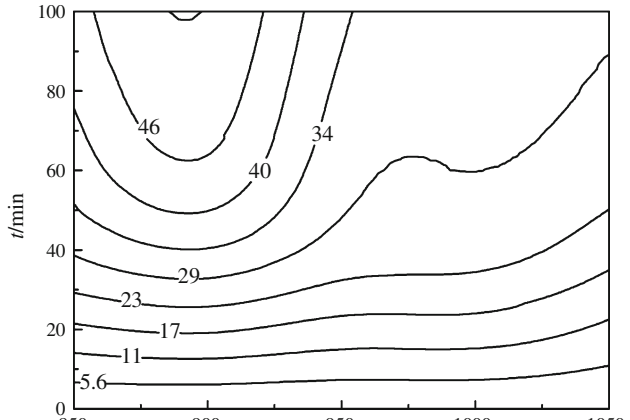

(b) Contour plot

Fig. 3 Effect of sulfation temperature and reaction time on sulfation conversion of limestone. **a** Surface plot and **b** Contour plot

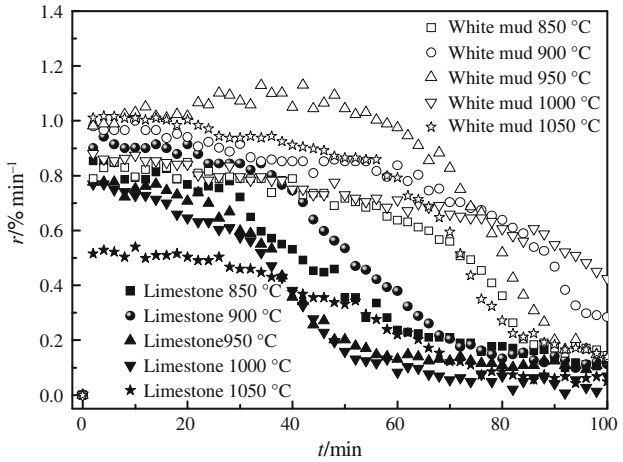

Fig. 4 Sulfation rates of white mud and limestone at the different sulfation temperatures

than at other sulfation temperatures. The white mud as SO_2 sorbent is more appropriate for the fluidized bed boiler with the combustion temperature above 920 °C. CaO derived from the white mud displays higher sulfation conversion than that derived from the limestone at the same reaction conditions. For example, the sulfation conversions at 950 °C and after 60 min for CaO derived from the white mud and the limestone are 63 and 32%, respectively.

Figure 4 plots the sulfation rates of CaO derived from the white mud and the limestone at the different sulfation temperatures. The sulfation rate of the sorbent is defined as follows.

$$r = \frac{\mathrm{d}X}{\mathrm{d}t} \tag{4}$$

The sulfation rates of CaO derived from the two sorbents decrease with the reaction time due to increase in $CaSO_4$ product layer. CaO derived from the white mud exhibits greater sulfation rate than that derived from the limestone at the same sulfation temperature. For instance, the sulfation rate of CaO derived from the limestone is very low less than 0.21% min^{-1} after 70 min, while that derived from the white mud is above 0.55% min^{-1}. It indicates that the white mud possesses better SO_2 capturing activity than the limestone at fluidized bed combustion temperatures.

Sulfation kinetics

The shrinking unreacted core model was used to describe the sulfation kinetics of calcium-based sorbent [21–23]. The calcium oxide derived from limestone is thought to be consisting of numerous solid particles which are considered to be small but dense grains. The reaction initiates on the grain surface in early stages which is called the chemical reaction-controlled stage. A layer of $CaSO_4$ products is formed around each CaO grain that separates the reaction surface of the solid from gas reactant with the reaction going on. The gas molecules have to diffuse through the product layer to the reaction surface. And then the sulfation reaction shifts to the product layer-diffusion-controlled stage [24]. Here, we still employ the shrinking unreacted core model to simulate the sulfation behavior of the white mud with the reaction time and analyze its sulfation kinetics. And the difference between the white mud and the limestone in sulfation kinetics is also compared.

The model in this investigation assumes negligible mass transfer through the gas film and isothermal conditions in the reactor [25]. If the chemical reaction is the rate-limiting step, the relationship between the reaction time and the sulfation conversion is given as

$$t = S_1 G(X) \tag{5}$$

$$S_1 = \frac{\rho_p R_p}{\alpha k C_{A0}} \tag{6}$$

If the diffusion through the product layer is the rate-limiting step, the relationship is shown as follows

$$t = S_2 P(X), \tag{7}$$

$$S_2 = \frac{\rho_p R_p^2}{6\alpha D_s C_{A0}} \tag{8}$$

where S_1 and S_2 is parameters in Eqs. 5 and 7, min; $G(X)$ and $P(X)$ is function defined by Eqs. 5 and 7, dimensionless; ρ_p is sorbent density, g cm^{-3}; R_p is radius of unreacted core for single CaO particle, cm; k is kinetic parameters, cm min^{-1}; C_{A0} is concentration of SO_2, mol cm^{-3}; D_s is effective diffusivity, cm^2 min^{-1}; α is stoichiometric coefficient of solid reactant, $\alpha = 1$. $G(X)$ and $P(X)$ are two functions related to the sulfation conversion as follows:

$$G(X) = 1 - (1 - X)^{1/3} \tag{9}$$

$$P(X) = 1 - 3(1 - X)^{2/3} + 2(1 - X) \tag{10}$$

k and D_s can be calculated according to Arrhenius' law as follows

$$k = k_0 \exp\left(-\frac{E_a}{RT}\right) \tag{11}$$

$$D_s = D_0 \exp\left(-\frac{E_p}{RT}\right) \tag{12}$$

where k_0 is pre-exponential factor, cm min^{-1}; D_0 is effective diffusivity at external grain surface, cm^2 min^{-1}; E_a is chemical reaction activation energy, kJ mol^{-1}; E_p is activation energy for product layer diffusion, kJ mol^{-1}; R is gas constant, 8.314 J mol^{-1} K^{-1}; T is sulfation temperature, K.

Incorporating Eqs. 6 and 8, we get the new equations by taking the logarithm of both sides in Eqs. 11 and 12 as follows

$$\ln\frac{1}{S_1} = \ln k_0 + \ln\frac{C_{A0}}{\rho_p R_p} - \frac{E_a}{RT} \tag{13}$$

$$\ln\frac{1}{S_2} = \ln D_0 + \ln\frac{6C_{A0}}{\rho_p R_p^2} - \frac{E_p}{RT} \tag{14}$$

The physical property parameters such as ρ_p and R_p are difficult to know due to the heterogeneous structure. Therefore, these parameters are assumed constant at different temperatures. The shrinking unreacted core model is determined by k_0, E_a, D_0, and E_p in different reaction stages, so these parameters for the white mud and the limestone must be calculated according to the experiment data.

$G(X)$-t in Eq. 5 and $P(X)$-t in Eq. 7 are related linearly, respectively. X is obtained from Fig. 3. Plots of $G(X)$-t and $P(X)$-t are shown in Figs. 5 and 6, respectively. And the solid lines obtained from linear fitting refer to the slopes of $G(X)$-t and $P(X)$-t. The correlation coefficient for the linear fit of $G(X)$-t is between 0.973 and 0.998, and that of $P(X)$-t is between 0.948 and 0.998. It indicates that the shrinking unreacted core model is appropriate to describe the sulfation kinetics of the white mud and the limestone. S_1 and S_2 are the slope coefficients of the fitting lines for $G(X)$-t and $P(X)$-t, so S_1 and S_2 is easily determined. $\ln 1/S_1 - 1/T$ in Eq. 13 and $\ln 1/S_2 - 1/T$ in Eq. 14 are related linearly, respectively. Thus, k_0, E_a, D_0, and E_p can be all calculated as demonstrated in Table 2. k and D_s are also obtained according to Eqs. 11 and 12 as shown in Table 3.

The reaction time of the white mud in chemical reaction controlling stage is longer than that of the limestone in the same reaction stage, as plotted in Fig. 5. The white mud exhibits higher values of k_0 and E_a than the limestone in the

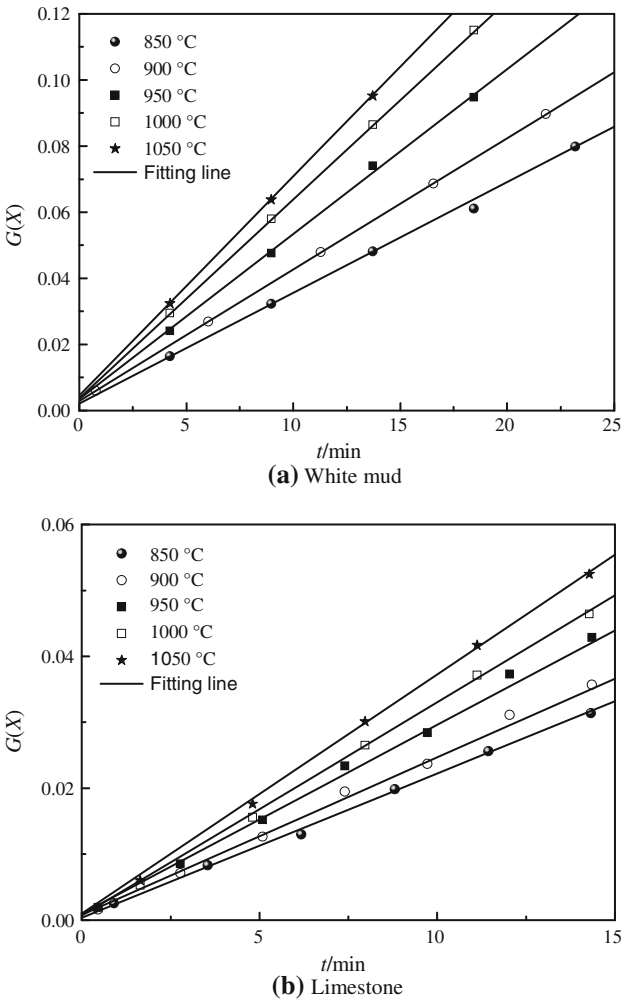

Fig. 5 Plots of the function G(X) vs. t for the sorbents in chemical reaction controlling stage. **a** White mud and **b** Limestone

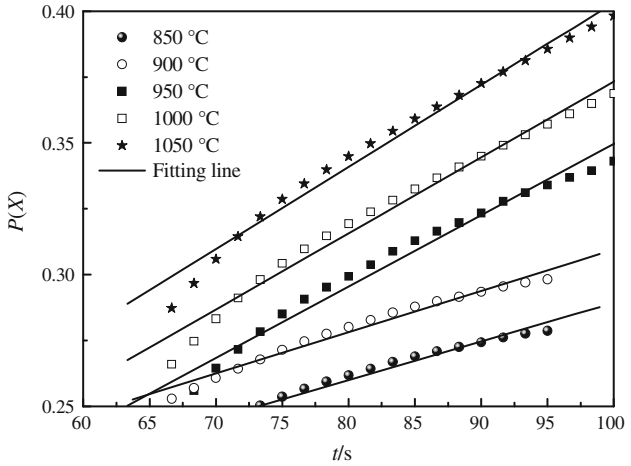

(a) White mud

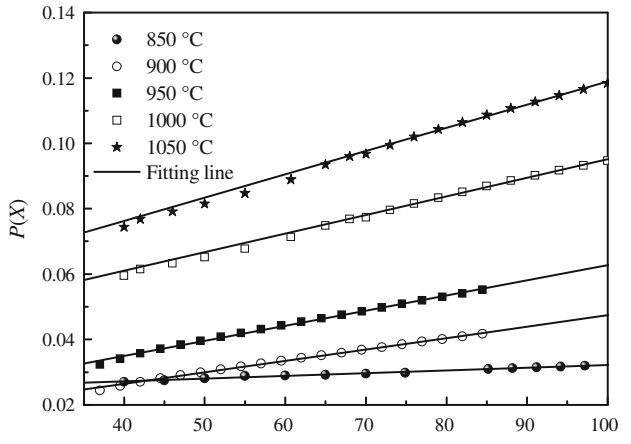

(b) Limestone

Fig. 6 Plots of the function $P(X)$ vs. t for the sorbents in product layer diffusion stage. **a** White mud and **b** Limestone

Table 2 Activation energy and pre-exponential factor

Sample	E_a/kJ mol^{-1}	k_0/cm min^{-1}	E_p/kJ mol^{-1}	D_0/cm^2 min^{-1}
White mud	44.94	565.10	55.61	2.62
Limestone	27.56	89.00	156.07	10784.42

chemical reaction controlling stage, while the former shows lower D_0 and E_p than the latter in the product layer diffusion stage. However, it is difficult to appraise the difference in the sulfation behavior of the two sorbents only depending on the values of k_0, E_a, D_0, and E_p due to the compensating effect in the sulfation. The kinetic parameter k and effective diffusivity D_s should be known at the different sulfation temperatures in order to understand the sulfation kinetics of the white mud and the limestone. k for the white mud is higher than that for the limestone as shown in Table 3. It shows that the white mud possesses a

Table 3 Sulfation kinetic parameters for white mud and limestone

Parameter	T/°C	White mud	Limestone
k/cm min^{-1}	850	4.6	4.0
	900	5.6	5.3
	950	6.8	5.8
	1000	8.1	6.6
	1050	9.5	7.3
$D_s \times 10^{-3}$/cm^2 min^{-1}	850	6.78	0.59
	900	8.74	1.21
	950	11.03	2.33
	1000	13.68	4.25
	1050	16.68	7.43

better sulfation activity than the limestone in the chemical reaction controlling stage. D_s for the white mud is also larger than that for the limestone in the product layer diffusion stage. It suggests that the white mud holds higher SO_2 diffusion and calcium cation diffusion capacity through $CaSO_4$ product layer than the limestone. The white mud contains more potassium and sodium ions than the limestone as presented in Table 1. Wu et al. [24] thought the addition of alkali metal ions to CaO can improve the calcium cation diffusion. Therefore, the white mud possesses greater calcium cation diffusion than limestone.

Microstructure analysis

Figure 7 demonstrates the surface areas of the white mud and the limestone after the calcination. The physical properties of a calcine depend largely on the calcination conditions (e.g. temperature, time, and atmosphere) and on the presence of impurities in the calcium-based sorbent

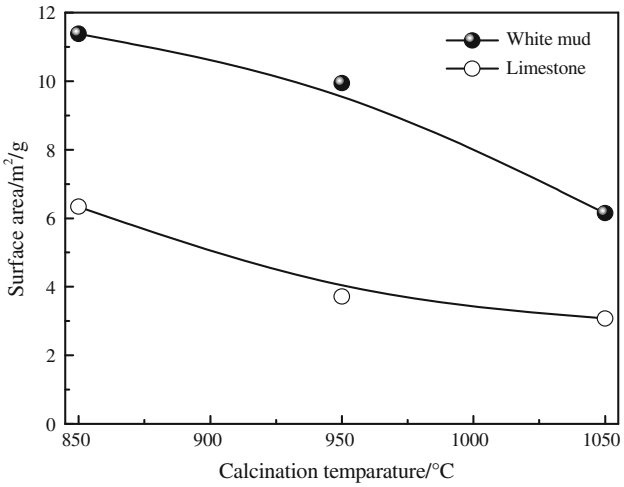

Fig. 7 Surface areas of white mud and limestone after calcination (calcination time 10 min)

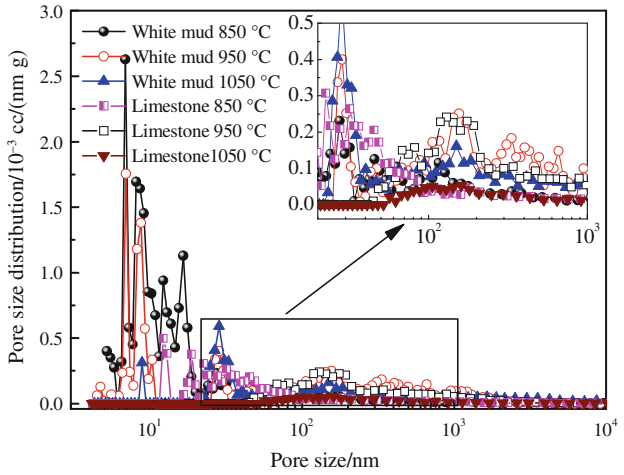

Fig. 8 Pore size distributions of white mud and limestone after calcination (calcination time 10 min)

[26–29].The surface areas for the two calcined sorbents decrease with increasing the calcination temperature from 850 to 1050 °C. Higher calcination temperature aggravates the sintering of the calcined sorbents. However, the surface area of the calcined white mud is approximately twice as large as the calcined limestone at the same calcination temperature. The calcined white mud at 1050 °C is almost equal to the calcined limestone at 850 °C in the surface area.

The calcines with large surface area and pore volume are the most reactive, because the rate of gas–solid reactions is determined primarily by the total area accessible to the gas and by the space available for the reaction product [26]. Laursen et al. [30] also thought that the calcium utilization and the sulfation pattern of calcium-based sorbents depended on the morphology and microstructure of the calcined sorbents. Higher surface area is beneficial to the sulfation of the sorbents, so the white mud exhibits better SO_2 capture behavior than the limestone.

The pore size distributions of the calcined white mud and the calcined limestone at different temperatures are exhibited in Fig. 8. The pores of calcined white mud at 850 and 950 °C dominantly distribute in 4–24 nm sizes. Also at 950 °C, the calcined white mud possesses the abundant pores in 24–263 nm sizes. When the temperature increases to 1050 °C, pores of the calcined white mud mainly lie in 24–498 nm sizes because the sintering at higher temperature induces a abrupt drop in the pores less than 24 nm sizes. The pore distribution of the calcined limestone is different from that of the calcined white mud. The pores of the calcined limestone at 850 °C mainly range from 17 to 312 nm, while its pores at 950 and 1050 °C dominantly distribute in 44.7–342 nm sizes. Mahuli et al. [31] proposed that the calcium-based sorbents could reach the maximum sulfation capacity when the pores of their calcines distributed predominantly in the 5–20 nm sizes. The pores of the white mud for calcination below 950 °C are dominant in the optimum pore size range, but few pores of the calcined limestone are in that range. Therefore, it is also a reason why the sulfation conversion of the white mud is higher than that of the limestone.

Conclusions

The white mud from paper manufacture was proposed as SO_2 sorbent for fluidized bed boiler. The calcination temperature above 850 °C is beneficial to the rapid decomposition of the white mud. The difference in calcination behavior of the white mud and the limestone is attributed to their different components. CaO derived from the white mud exhibits the maximum sulfation conversion of 83% at about 940 °C, and the sulfation conversion can reach above 76% at the range of 890–980 °C. CaO derived from the limestone achieves the highest conversion of 50% at approximately 880 °C and can retain higher conversion above 45% at 850–920 °C than at other sulfation temperatures. The white mud is more appropriate for SO_2 removal than the limestone at the fluidized bed combustion temperature above 920 °C. CaO derived from the white mud displays higher sulfation conversion than that derived from the limestone at the same reaction conditions. It indicates that the shrinking unreacted core model is appropriate to describe the sulfation kinetics of the white mud. The reaction time of the white mud in chemical reaction controlling stage is longer than that of the limestone in the same reaction stage. k for the white mud is higher than that for the limestone. D_s for the white mud is also larger than that for the limestone in the product layer diffusion stage. It suggests that the white mud holds higher SO_2 diffusion and calcium cation diffusion capacity through $CaSO_4$ product layer than the limestone. The surface area of the calcined white mud is approximately twice as large as the calcined limestone at the same calcination temperature. The pores of the calcined white mud below 950 °C dominantly distribute in 4–24 nm range which is almost optimum pore size for sulfation of calcium-based sorbents. That is a reason why the white mud shows better sulfation capacity than the limestone.

Acknowledgements This study was financially supported by Research Fund for the Doctoral Program of Higher Education of China (20100131120055).

References

1. Livraghi S, Paganini MC, Giamello E. SO_2 reactivity on the MgO and CaO surfaces: a CW-EPR study of oxo-sulphurradical anions. J Mol Catal. 2010;322:39–44.

2. Sakizci M, Alver BE, Yorukogullari E. Thermal and SO_2 adsorption properties of some lays from Turkey. J Therm Anal Calorim. 2011;103:435–41.
3. Trikkel A, Zevenhoven R, Kuusik R. Modelling SO_2 capture by Estonian limestones and dolomites. Proc Est Acad Sci Chem. 2000;49:53–70.
4. Crnkovic PM, Milioli FE, Pagliuso JD. Kinetics study of the SO_2 sorption by Brazilian dolomite using thermogravimetry. Thermochim Acta. 2006;447:161–6.
5. Anthony EJ, Bulewicz EM, Jia L. Reactivation of limestone sorbents in FBC for SO_2. Prog Energy Combust Sci. 2007;33:171–210.
6. Trikkel A, Keelmann M, Kaljuvee T. CO_2 and SO_2 uptake by oil shale ashes: effect of pre-treatment on kinetics. J Therm Anal Calorim. 2010;99:763–9.
7. Kaljuvee T, Toom M, Trikkel A, Kuusik R. Reactivity of oil shale ashes in the binding of SO_2. J Therm Anal Calorim. 2007;88:51–8.
8. Kaljuvee T, Trikkel A, Kuusik R. Decarbonization of natural lime-containing materials and reactivity of calcined products towards SO_2 and CO_2. J Therm Anal Calorim. 2001;64:1229–40.
9. Robertson A, Goidich S, Fan Z. 1300°F 800 MWe USC CFB boiler design study. In: Proceedings of the 20th International Conference on Fluidized Bed Combustion, Xian, China; 2009, p. 125–31.
10. Liu W, Yang J, Xiao B. Review on treatment and utilization of bauxite residues in China. Int J Miner Process. 2009;93:220–31.
11. Gorai B, Jana RK. Premchand, Characteristics and utilization of copper slag-review. Resour Conserv Recycl. 2003;39:299–313.
12. Wang SB, Ang HM, Tade MO. Novel applications of red mud as coagulant, adsorbent and catalyst for environmentally benign processes. Chemosphere. 2008;72:1621–35.
13. Yamada K, Harato F. SO_2 removal from waste-gas by red mud slurry pilot test and operation results of the plant. Kagaku Kogaku Ronbun. 1982;8:32–8.
14. Fan HL, Li CH, Xie KC. Testing of iron oxide sorbent for high-temperature coal gas desulfurization. Energy Sour. 2005;27:245–50.
15. Cheng J, Zhou JH, Liu JZ, Cao XY, Cen KF. Physicochemical characterizations and desulfurization properties in coal combustion of three calcium and sodium industrial wastes. Energy Fuels. 2009;23:2506–16.
16. Lin S, Luo HJ. Preparation of soil nutrient amendment using white mud produced in ammonia-soda process and its environmental assessment. Trans Nonferrous Met Soc China. 2009;19:1383–8.
17. Zhu MX, Lee L, Wang HH, Wang Z. Removal of an anionic dye by adsorption/precipitation processes using alkaline white mud. J Hazard Mater. 2007;149:735–41.
18. Laursen K, Grace JR, Lim CJ. Enhancement of the sulfur capture capacity of limestones by addition of the Na_2CO_3 and NaCl. Environ Sci Technol. 2001;35:4384–9.
19. Laursen K, Kern AA, Grace JR, Lim CJ. Characterization of the enhancement effect of Na_2CO_3 on the sulfur capture capacity of limestones. Environ Sci Technol. 2003;37:3709–15.
20. Siagi ZO, Mbarawa M, Mohamed AR, Lee KT, Dahlan I. The effects of limestone type on the sulphur capture of slaked lime. Fuel. 2007;86:2660–6.
21. Stanmore BR, Gilot P. Review-calcination and carbonation of limestone during thermal cycling for CO_2 sequestration. Fuel Process Technol. 2005;86:1707–43.
22. Anthony EJ, Granatstein DL. Sulfation phenomena in fluidized bed combustion systems. Prog Energy Combust Sci. 2001;27:215–36.
23. Li RY, Qi HY, You CF, Xu XC. Kinetic model of CaO/fly ash sorbent for flue gas desulphurization at moderate temperatures. Fuel. 2007;86:785–92.
24. Wu ZH, Kou P, Yu ZW. The modulation of desulphurization properties of calcium oxide by alkali carbonates. J Therm Anal Calorim. 2002;67:745–50.
25. Mohamed AR. Kinetic model for the reaction between SO_2 and coal fly ash/CaO/$CaSO_4$ sorbent. J Therm Anal Calorim. 2005;79:691–5.
26. Chrissafis K. Multicyclic study on the carbonation of CaO using different limestones. J Therm Anal Calorim. 2007;89:525–9.
27. Chrissafis K, Paraskevopoulos KM. The effect of sintering on the maximum capture efficiency of CO_2 using a carbonation/calcination cycle of carbonate rocks. J Therm Anal Calorim. 2005;81:463–8.
28. Chrissafis K, Dagounaki C, Paraskevopoulos KM. The effects of procedural variables on the maximum capture efficiency of CO_2 using a carbonation/calcination cycle of carbonate rocks. Thermochim Acta. 2005;428:193–8.
29. Wieczorek-Ciurowa K. Peculiarities of interactions in the $CaCO_3$/CaO-SO_2/SO_3-air system. J Therm Anal Calorim. 1998;53:649–58.
30. Laursen K, Duo W, Grace JR, Lim CJ. Sulfation and reactivation characteristics of nine limestones. Fuel. 2000;79:153–63.
31. Mahuli SK, Agnihotri R, Chauk S, Ghosh-Dastidar A, Wei SH, Fan LS. Pore-structure optimization of calcium carbonate for enhanced sulfation. AIChE J. 1997;43:2323–35.